Power Losses in Long String and Parallel-Connected Short Strings of Series-Connected Silicon-Based Photovoltaic Modules Due to Partial Shading Conditions

Anssi Mäki, *Student Member, IEEE*, and Seppo Valkealahti, *Member, IEEE*

***Abstract*—Configuration of a photovoltaic (PV) power generator has influence on the operation of the generator, especially if it is prone to partial shading. In this paper, the mismatch losses and the power losses due to failure in tracking of the global maximum power point of a long string of 18 series-connected PV modules and three short strings of six series-connected PV modules connected in parallel are investigated under different partial shading conditions by using a MATLAB Simulink simulation model. The generators with parallel-connected short strings are studied in case when they have the same operating voltage and when they operate as separate strings. The results show that long series connection of modules and parallel connections of strings via a single inverter to the electrical grid should be minimized to avoid losses in case of partial shading conditions. Under partial shading conditions, short strings operating separately have the lowest power losses.**

***Index Terms*—Grid-connected photovoltaic power generator, mismatch losses, photovoltaic cells, photovoltaic systems, solar energy, solar power generation.**

I. Introduction

GLOBAL warming and the limited resources of fossil fuels have increased the need for renewable energy [1]–[3]. Solar radiation is the largest source of renewable energy [4], [5] and the only one by which the present primary energy consumption can be replaced.

Photovoltaic (PV) power generators convert the energy of solar radiation directly to electrical energy without any moving parts. PV power generators can be classified into stand-alone and grid-connected generators [6]. In stand-alone systems, the energy storage has big influence on the design of the systems. In grid-connected systems, the grid acts as an energy storage into which the PV power generator can inject power whenever power is available.

The electrical grids have specific voltage levels. They are much higher than the maximum voltage of a single silicon-based PV cell. In order to interface PV power generators with the grid, the PV cells are connected in series to form PV modules. The voltage of an individual PV module is normally still too low to be conveniently used as a grid-connected PV power generator. Therefore, the generators are built by connecting PV modules in series and in parallel in order to get a sufficient voltage level and to increase the nominal power of the generator.

The series connection of PV cells is prone to mismatch power losses if the electrical characteristics of the PV cells are not similar or the cells do not operate under uniform conditions. The PV cell with the lowest short-circuit (SC) current limits the current of the whole series connection [7]. SC currents of the PV cells can vary due to various technical or environmental reasons. Technical reasons can be minimized during the manufacture of PV modules and during system design phase, but environmental reasons are harder to avoid.

One major environmental reason for uneven SC currents is partial shading of the PV power generator due to clouds, trees, buildings, etc. Under partial shading conditions, for example, if one PV cell of the generator composed of series-connected cells is shaded, the SC currents of the non-shaded cells are higher than the SC current of the shaded cell. If then the current of the PV power generator is higher than the SC current of the shaded cell, the shaded cell will be reverse biased due to the other cells in the series connection. In this case, the reverse biased cell acts as a load in the series connection dissipating part of the power generated by the other cells leading to power losses. This can also lead to hot spots in the shaded cell and the cell can be damaged [8]. The worst situation is when the series connection is short circuited. Then, the shaded cell dissipates all of the power generated by the other cells in the series connection.

In order to prevent PV cells from damaging due to hot spots, manufacturers of PV modules have connected bypass diodes in antiparallel with PV cells [9]. There is a total amount of 54 series-connected PV cells in a typical PV module designed to be used in grid-connected PV power generators with three bypass diodes, each of them connected in antiparallel with 18 PV cells. When some of the PV cells of the PV module become shaded, they become reverse biased and the bypass diode connected in antiparallel starts to bypass the current exceeding the SC current of the shaded cells and limits the power dissipated in the shaded cells.

Under nonuniform conditions when a part of the bypass diodes starts to conduct, the power–voltage (*P–U*) curve of the PV module shows multiple maxima as illustrated in Fig. 9 in which there are *P–U* curves of a PV power generator called

Manuscript received June 22, 2011; revised October 19, 2011; accepted November 7, 2011. Date of publication December 13, 2011; date of current version February 17, 2012. Paper no. TEC-00308-2011.

The authors are with the Department of Electrical Energy Engineering, Tampere University of Technology, Tampere FI-33101, Finland (e-mail: anssi.maki@tut.fi; seppo.valkealahti@tut.fi).

Digital Object Identifier 10.1109/TEC.2011.2175928

"Parallel strings generator" operating under partial shading conditions. In this case, extraction of maximum power from the PV power generator is not straightforward, because there is one local maximum power point (MPP) at low voltages and another at high voltages. Typically used maximum power point tracking (MPPT) algorithms are based on the hill climbing method [10], [11], which drives the operating point just to the nearest maximum of the *P–U* curve. They can fail to track the MPP with highest power, the global MPP, when the generator is operating under partial shading conditions. In this case, in addition to mismatch losses, there are also losses due to tracking of a local MPP with lower power instead of the global MPP. Algorithms to track the global MPP in the case of multiple maxima have also been developed, e.g., in [12] and [13], but they tend to be complicated and many of them are unable to track the global MPP under all nonuniform conditions.

Significant effects of partial shading on the electrical characteristics and the energy yield of PV power generators in different generator configurations have been reported by several authors [14]–[25]. In many of these papers, the focus has been on the development of a simulation model for series-connected PV modules and, therefore, only a few current–voltage (*I–U*) or *P–U* curves have been provided in order to give an idea of the operation of the simulation model and the PV power generator in specific nonuniform conditions. Comparably, in many papers, the focus has been on studying the operation of an MPPT algorithm or an interfacing device. Therefore, we are still short of a comprehensive knowledge about the effects of nonuniform conditions on different PV power generator configurations.

In this paper, the mismatch losses and power losses due to the tracking of a local MPP instead of the global one have been studied. A long string of 18 series-connected PV modules and three short strings of six series-connected PV modules connected in parallel are investigated under different partial shading conditions by using a MATLAB Simulink simulation model. The operation of short strings has been studied in case when strings are connected in parallel and have the same operating voltage and in case when they operate as separate strings. In the simulations, the number of shaded modules and the shading strength have been varied from 0% to 100%.

Typically, the configurations of PV power generators have been named based on the interfacing device used to connect the generators to the electrical grid [25]–[27]. In this paper, the Long string generator corresponds to the string inverter configuration, the Parallel strings generator to the central inverter configuration, and the Multi-string generator to the multi-string inverter configuration.

II. Simulation Model

The model of a PV module presented by Villalva *et al*. [28] has been used to simulate the operation of a PV power generator. The model is based on the well-known one-diode model of a PV cell [29] shown in Fig. 1. It provides the following relation between the current I and the voltage U of a PV cell:

$$I = I_{\rm ph} - I_{\rm o}\left[\exp\left(\frac{U + R_{\rm s}I}{AU_{\rm t}}\right) - 1\right] - \frac{U + R_{\rm s}I}{R_{\rm sh}} \quad (1)$$

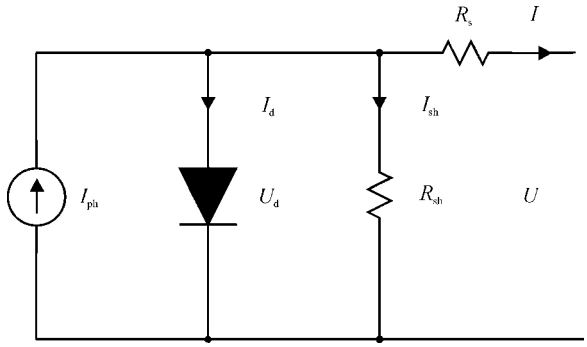

Fig. 1. One-diode model of a PV cell.

where $I_{\rm ph}$ is the light-generated current, $I_{\rm o}$ is the dark saturation current, $R_{\rm s}$ is the series resistance, $R_{\rm sh}$ is the shunt resistance, A is the ideality factor, and $U_{\rm t}$ is the thermal voltage of the PV cell. $I_{\rm d}$ and $U_{\rm d}$ in Fig. 1 are the current and voltage of the diode, respectively. $I_{\rm d}$ represents the second term in the right-hand side of (1) and $U_{\rm d} = U + R_{\rm s}I$. The last term in the right-hand side of (1) is the current through the shunt resistance and is marked with $I_{\rm sh}$ in Fig. 1.

The simulation model of a PV module can be obtained by scaling the parameters used in the one-diode model for one cell by the number of series-connected PV cells in the module. The thermal voltage of the PV module is given by $U_{\rm t} = N_{\rm s}kT/q$, where $N_{\rm s}$ is the number of cells in the module, k is the Boltzmann constant, T is the temperature of the module, and q is the elementary charge.

It can be seen in Fig. 1 that the light-generated current $I_{\rm ph}$ can be obtained as a function of SC current in any environmental conditions by current division by assuming that in SC condition the diode current $I_{\rm d}$ is negligible and almost all of the light-generated current flows to the terminals of the module. Accordingly

$$I_{\rm ph} = (I_{\rm SC,STC} + K_{\rm i}\Delta T)\frac{G}{G_{\rm STC}}\frac{R_{\rm sh} + R_{\rm s}}{R_{\rm sh}} \quad (2)$$

where $I_{\rm SC,STC}$ is the SC current in standard test conditions (STC), $K_{\rm i}$ is the temperature coefficient of the SC current, G is the irradiance reaching the surface of the module, and $\Delta T = T - T_{\rm STC}$, where T is the temperature of the PV module. In STC, the spectral conditions are AM1.5, the module temperature $T_{\rm STC}$ is 25 °C, and the irradiance $G_{\rm STC}$ 1000 W/m^2.

The dark saturation current $I_{\rm o}$ depends on the temperature, structure, and material of the PV cell. It is obtained by solving (1) in open-circuit (OC) condition. When the effect of temperature on the OC voltage is added, the dark saturation current is given by

$$I_{\rm o} = \frac{I_{\rm ph} - (U_{\rm OC,STC} + K_{\rm u}\Delta T)/R_{\rm sh}}{\exp((U_{\rm OC,STC} + K_{\rm u}\Delta T)/(AU_{\rm t})) - 1} \quad (3)$$

where $U_{\rm OC,STC}$ is the OC voltage in STC and $K_{\rm u}$ is the temperature coefficient of the OC voltage.

The temperature of the PV module is assumed to depend linearly on irradiance

$$T = T_{\rm amb} + K_{\rm t}G \quad (4)$$

where T_{amb} is the ambient temperature. The temperature-rise coefficient K_{t} is obtained by using the nominal operating cell temperature (NOCT) given by the manufacturer. NOCT is defined in conditions in which the irradiance is 800 W/m^2, ambient temperature is 20 °C, and wind speed is less than 1 m/s with free air access to the rear of the module. NOCT of the PV cells is 46 °C for NAPS NP190GKg PV modules used to verify our theoretical model. The NOCT operating conditions were used for ambient temperature and wind speed in the simulations. The operation of the PV power generators in this paper have been modeled by using (1)–(4).

A method to obtain the series and the shunt resistances is also introduced by Villalva *et al*. [28]. It is based on the OC voltage, the SC current, and the MPP in the electrical characteristics of the PV module. The ideality factor A of 1.3 is used as a typical value found in the literature for silicon-based PV modules [28], [30]. It has been pointed out in [28] that there is only one pair of values for R_{s} and R_{sh} for which the MPP of the model coincides with the given MPP for a specific PV module in STC. This pair of values can be obtained from

$$P_{\mathrm{MPP,STC}} = U_{\mathrm{MPP,STC}} \left\{ I_{\mathrm{ph,STC}} - I_{\mathrm{o,STC}} \left[\exp\left(\frac{U_{\mathrm{MPP,STC}} + R_{\mathrm{s}} I_{\mathrm{MPP,STC}}}{A U_{\mathrm{t,STC}}} \right) - 1 \right] - \frac{U_{\mathrm{MPP,STC}} + R_{\mathrm{s}} I_{\mathrm{MPP,STC}}}{R_{\mathrm{sh}}} \right\} \quad (5)$$

where $P_{\mathrm{MPP,STC}}$ is the power, $U_{\mathrm{MPP,STC}}$ is the voltage, and $I_{\mathrm{MPP,STC}}$ is the current of the module at MPP in STC. The light-generated current in STC $I_{\mathrm{ph,STC}}$ can be obtained from (2) by inserting $\Delta T = 0$ K and $G = G_{\mathrm{STC}}$. The shunt resistance R_{sh} can be obtained from (5) as a function of series resistance R_{s} as shown in (6) at the bottom of this page.

Although the equation for light-generated current $I_{\mathrm{ph,STC}}$ includes both the series and the shunt resistances and the equation for dark saturation current includes the shunt resistance as shown in (2) and (3), it is still possible to explicitly solve (6) with respect to R_{sh} as a function of series resistance R_{s}. The pair of resistances is solved iteratively by using a typical series resistance of the PV module as a starting point and finding the pair for which the maximum power in STC is exactly the same as given by the manufacturer of a PV module under investigation. By using this method, the electrical characteristics of the modeled PV module can be made to match the OC, SC, and MPP points of the *I–U* characteristic in STC. The temperature and irradiance in other operating conditions are taken into account as shown in (2)–(4).

The operation of bypass diodes used in the PV module to protect the cells against hot spots is modeled by (1) by assuming the shunt resistance R_{sh} of the diode to be infinite and the light-generated current I_{ph} to be zero. The rest of the parameters in (1), such as the diode ideality factor A_{bypass}, series resistance $R_{\mathrm{s,bypass}}$, and diode dark saturation current $I_{\mathrm{o,bypass}}$, are obtained by means of curve fitting to a measured *I–U* characteristic of a Schottky diode. The parameters are given in Table I. In simulations, the current of the bypass diode connected in antiparallel with shaded cells is the current exceeding to SC current of the shaded cells.

TABLE I
PARAMETERS FOR BYPASS DIODES

Parameter	Value
$R_{\mathrm{s,bypass}}$	0.02 Ω
A_{bypass}	1.50
$I_{\mathrm{o,bypass}}$	3.20 μA

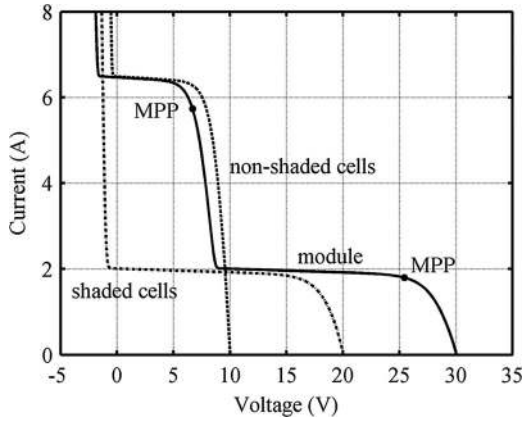

Fig. 2. *I–U* characteristics of a PV module operating under partial shading conditions with two-thirds of the cells shaded.

The electrical behavior of a PV module composed of 54 PV cells and three bypass diodes, each of them connected in antiparallel with 18 PV cells, is illustrated in Fig. 2 under partial shading conditions. Two blocks of 18 PV cells with bypass diodes connected in antiparallel are shaded and one block is non-shaded. *I–U* curves of the shaded and non-shaded cells are shown in addition to the *I–U* curve of the whole PV module in order to illustrate the effect of bypass diodes on the electrical characteristic of a PV module under partial shading condition.

The effect of bypass diodes on the *I–U* curve of the PV module under partial shading condition can be seen in Fig. 2 at voltages below 10 V, where the current of the whole PV module is higher than the SC current of the shaded cells. In this region, the voltage of the whole module is the sum of the voltage of the non-shaded cells and the threshold voltages of the conducting bypass diodes (-1.2 V) connected in antiparallel with the shaded cells. At voltages above 10 V, the current of the PV module is lower than the SC current of the shaded cells, and therefore, the bypass diodes do not conduct current. In this case, the voltage of the module is just the sum of the voltages of the non-shaded and shaded cells.

$$R_{\mathrm{sh}} = \frac{U_{\mathrm{MPP,STC}}^2 + U_{\mathrm{MPP,STC}} I_{\mathrm{MPP,STC}} R_{\mathrm{s}}}{U_{\mathrm{MPP,STC}} I_{\mathrm{ph,STC}} - U_{\mathrm{MPP,STC}} I_{\mathrm{o,STC}} \left[\exp\left((U_{\mathrm{MPP,STC}} + I_{\mathrm{MPP,STC}} R_{\mathrm{s}}) / (A U_{\mathrm{t,STC}}) \right) - 1 \right] - P_{\mathrm{MPP,STC}}} \quad (6)$$

TABLE II
ELECTRICAL CHARACTERISTICS OF NAPS NP190GKG PV MODULE GIVEN BY THE MANUFACTURER IN STC

Parameter	Value
$U_{OC,STC}$	33.1 V
$I_{SC,STC}$	8.02 A
$P_{MPP,STC}$	190 W
$U_{MPP,STC}$	25.9 V
$I_{MPP,STC}$	7.33 A

TABLE III
PARASITIC RESISTANCES AND TEMPERATURE COEFFICIENTS FOR THE NAPS NP190GG PV MODULE USED IN THE SIMULATIONS

Parameter	Value
R_s	0.33 Ω
R_{sh}	188 Ω
A	1.30
K_u	-0.124 V/K
K_i	0.005 A/K
K_t	0.033 K/W/m^2

The used simulation model of the PV module and the generator is, naturally, a simplification of the operation of real modules and generators. For example, the light-generated current is dependent on the energy of the bandgap of the PV cell material and on the spectrum of the irradiance and not just on the value of irradiance as assumed in the model. Also, the PV modules are not exactly identical in actual generators. However, the used model is accurate enough for analyzing the phenomena studied in this paper.

The simulation model used in this paper has been fitted to the characteristic values of NAPS NP190GKg PV module. Basic electrical characteristics of the PV module given by the manufacturer have been presented in Table II. The module is composed of 54 series-connected PV cells with three bypass diodes, each of them connected in antiparallel with 18 series-connected PV cells. NAPS NP190GKg PV module, which is manufactured by using polycrystalline silicon PV cells, can be thought of as a typical PV module used in grid-connected PV power generators.

The method developed by Villalva *et al.* has been used to obtain the series and shunt resistances. Resistances and temperature-rise coefficient corresponding to NAPS NP190GKg PV module are shown in Table III. Typical values of temperature coefficients for OC voltage and SC current for silicon PV cells are used [30].

The operation of the simulation model can be seen in Fig. 3, in three different irradiance and temperature conditions. The irradiance of the module has been measured by using Kipp & Zonen SP Lite2 pyranometer, which was attached to the module frame and had the same tilt angle as the module. The temperature of the PV module was deduced from the measured irradiance, ambient temperature, and backplate temperature of the module. The ambient and backplate temperatures were measured by using Vaisala HMP155 temperature probe and a PT100 sensor, respectively.

The accuracy of the simulation model is sufficiently high, especially, under high irradiance conditions. This can be seen in Fig. 3 by comparing the simulated and measured *I–U* curves of the module in the case when irradiance is 729 W/m^2. The accuracy of the simulation model slightly decreases with decreasing irradiance as can be seen for 415- and 132-W/m^2 irradiances around the MPPs (the knees in the curves). The validity of the simulation model has been previously verified [21] also for Raloss SR30-36 PV modules manufactured by using monocrystalline silicon cells operating under partial shading conditions. Furthermore, the simulation model is in accordance with the results presented in [28].

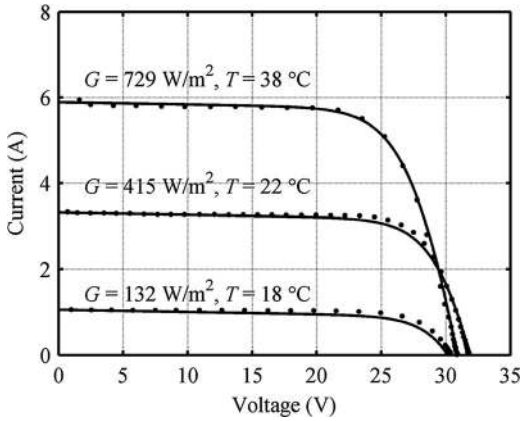

Fig. 3. Simulated and measured *I–U* characteristics of NAPS NP190GKg PV module under three different operating conditions. Simulated characteristics are drawn with solid lines and measured with dots.

In this paper, the basic behavior of power losses of different silicon-based PV power generator configurations is studied under partial shading conditions. The operation of a typical PV module used in grid-connected PV power generators has been the basis of the simulations. The results could slightly change if different PV modules would be used, but the basic general behavior will be the same for all silicon-based PV modules. Therefore, it can be concluded that the accuracy of the simulation model is sufficient for the studies in this paper.

III. SHADING OF PV GENERATORS

Three different PV power generators composed of 18 PV modules have been studied and are presented in Fig. 4. They are (a) the Long string generator composed of 18 series-connected PV modules, (b) the Parallel strings generator of three parallel-connected strings of six PV modules and blocking diodes connected in series, and (c) the Multi-string generator composed of three separately operated strings of six series-connected PV modules.

Characteristic values of NAPS NP190GKg PV modules have been used as reference values in our simulations. PV modules consists of 54 PV cells connected in series, which are protected against hot spots by three bypass diodes, each of them connected in antiparallel with 18 cells.

In simulations, shading of the generators has been done one-third of a PV module (18 PV cells protected by one bypass diode) at a time. The first five steps of the shading pattern in the case of Long string generator are illustrated in Fig. 5. In

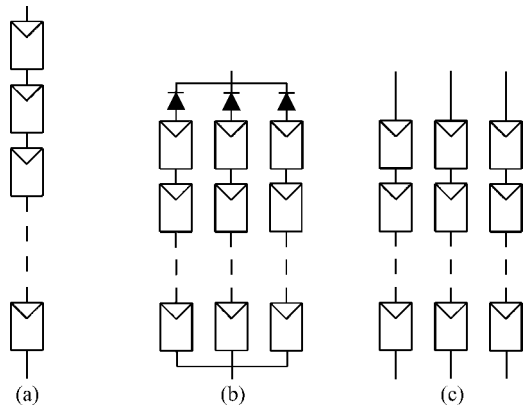

Fig. 4. Studied PV power generators: (a) Long string, (b) Parallel strings, and (c) Multi-string generators.

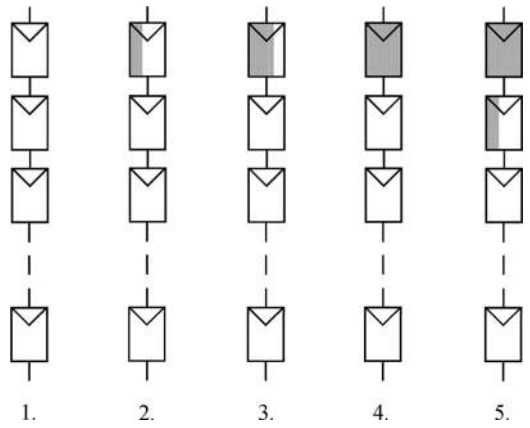

Fig. 5. Shading pattern of the Long string PV power generator used in simulations. Shaded parts of the generator are shown with gray color.

cases of Parallel strings and Multi-string generators, one string is completely shaded before shading the next string. In this way, the basic behavior of different configurations of PV power generators can be investigated. The effects of different partial shading conditions, for example, shading one-third of each PV string connected in parallel, can be deduced based on the shading pattern used in this paper.

IV. Results

In simulations, the main variables were the relative portion of shaded PV cells in the PV power generator (system shading) and the attenuation of irradiance due to the shading (shading strength). Shading strength is the amount of lost irradiance due to shading divided by the total irradiance without shading.

The simulated PV power generators were composed of 18 PV modules. Because the shading of the PV power generators was done one-third of a PV module at a time, the generators can be divided into 54 blocks of 18 series-connected PV cells with a bypass diode connected in antiparallel with the cells. In simulations, the amount of shaded blocks of the PV power generators (system shading) was varied from 0 to 54 (0 to 100%) yielding 55 different values for system shading.

The irradiance of the non-shaded blocks of the PV power generators was 800 W/m^2 corresponding to the NOCT conditions. In NOCT conditions, the irradiance is 800 W/m^2, ambient temperature is 20 °C, and wind speed is 1 m/s with free air access to the rear of the PV module [31]. The temperature of the modules in these conditions for NAPS NP190GKg PV module was 46 °C. The irradiance of the shaded blocks was varied from 0 to 800 W/m^2 with the same amount of discrete steps (55) than the system shading.

In case of 0% system shading, all the PV modules are non-shaded and the PV power generators operate under uniform conditions. Correspondingly, in case of 100% system shading, all the PV modules are shaded and the PV power generators again operate under uniform conditions. Furthermore, for shading strength of 0%, the PV power generators operate under uniform conditions regardless of the system shading, because the shading does not attenuate the irradiance. In case of 100% shading strength, the shaded blocks do not receive any irradiance and are not affecting the electrical characteristics of the generator except for the threshold voltage of the conducting bypass diodes. In these kinds of uniform shading conditions, the operation of PV power generators is straightforward following typical *I–U* characteristics of a PV cell.

In all other shading conditions than those mentioned earlier, partial shading affects the PV power generator *I–U* curve and can have serious consequences to the obtained power depending on the PV power generator configuration and on the operation of the device interfacing the generator with the electrical grid. In the following sections, we show how partial shading affects the global MPP power and causes mismatch losses and losses due to operation at a local MPP instead of the global one in the case of three basic PV power generator configurations shown in Fig. 4.

A. Power of the Global MPP

The *P–U* curves of the PV power generators under every simulated partial shading condition have been calculated, and the power of the highest MPP, i.e., the global MPP, has been saved in order to illustrate the effect of partial shading on the maximum power of the PV power generators. The power of the global MPP has been shown as a function of system shading and shading strength as contour graphs in Fig. 6 for the three investigated PV power generators.

The power of the global MPP decreases, naturally, if the system shading and/or shading strength increase as can be seen in Fig. 6. For the Long string generator, it can clearly be seen in Fig. 6(a) that there is a distinct turn on the contours near the diagonal from the origin to the top-right corner of the figure. Above the diagonal, the local MPP at low voltages is the global MPP, and below the diagonal, the local MPP at high voltages is the global MPP. As can be seen in Fig. 6(a), the contours are vertical when the local MPP at low voltages is the global MPP. This means that the power of the global MPP decreases linearly with increasing system shading, because the voltage of the global MPP is the sum of MPP voltages of individual non-shaded blocks and the threshold voltages of the conducting

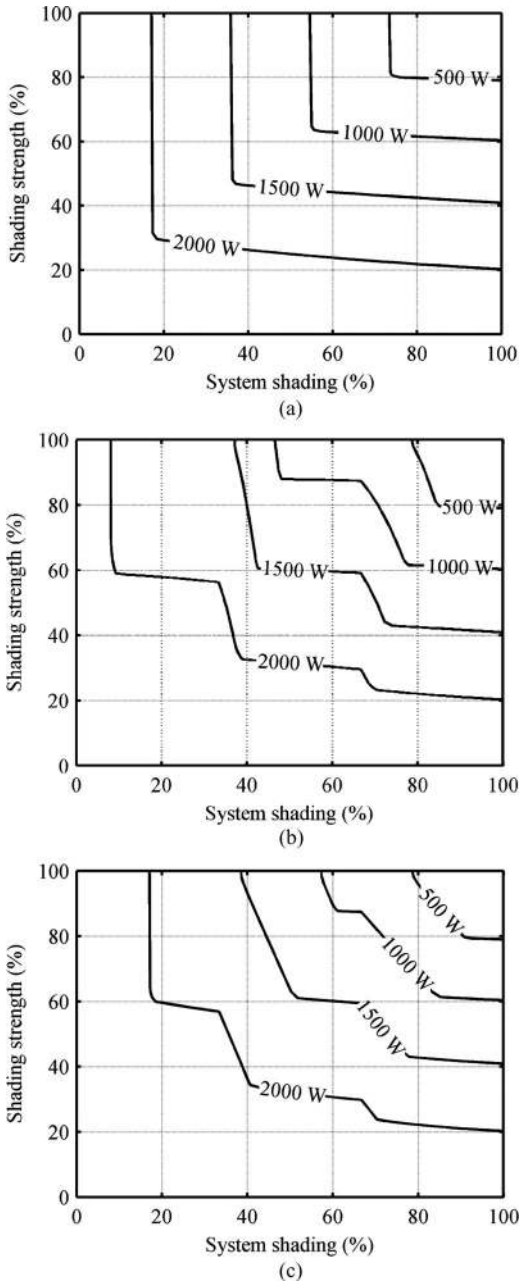

Fig. 6. Global MPP power as a function of system shading and shading strength for (a) Long string, (b) Parallel strings, and (c) Multi-string PV power generators.

bypass diodes. As can be seen in Fig. 6(a), the MPP at low voltages is usually the global MPP when shading strength is high. This can be presumed to be a common case, because typical shading strengths are around 80–85% on a clear sky day [32]. When the contours are horizontal, the local MPP at high voltages is the global MPP. In this kind of situations, the power of the global MPP decreases almost linearly with increasing shading strength, because the MPP current is linearly proportional to the irradiance while the voltage of the MPP remains almost unchanged.

Both the Parallel strings and Multi-string generators have three parallel-connected strings of six PV modules connected in series. Because of this basic configuration, their 2000-W global MPP contour graphs in Fig. 6(b) and (c) have three different vertical and horizontal sections. There are three different shading conditions where the local MPP at low voltages is the global MPP and three conditions where the local MPP at high voltages is the global MPP. Clear changes in the 2000-W curves take place at system shadings of 33.3% and 66.7%. At 33.3% system shading, one string is completely shaded and two other strings are non-shaded, and at 66.7%, two strings are completely shaded and one string is non-shaded. For both system shadings, the PV power generator has only one MPP, because each of the parallel strings operates under uniform conditions.

Turning points on the 2000-W contours in Fig. 6(a) and (b) for system shadings of 9%, 39%, and 70% for Parallel strings generator and 19%, 41%, and 70% for Multi-string generator are due the fact that the powers of the two local MPPs are equal due to a particular partial shading condition in the first, second and, finally, the third parallel string, respectively. This is basically the same phenomenon, which takes place only once for global MPP power contours in the case of Long string generator on the diagonal in Fig. 6(a).

The 1500-W global MPP power contour of the Long string PV generator in Fig. 6(a) corresponds to the case when over 33.3% of the string is shaded. This means that in the case of Parallel strings or Multi-string PV generators, the first parallel string is fully shaded and only strings two and three cause turns to the 1500-W power contours as shown in Fig. 6(b) and (c). The same phenomenon takes place at 1000 W. At 500 W, two strings are fully shaded and turns on the contours are due to partial shading of the third string.

Based on the global MPP power contour graphs in Fig. 6, the Multi-string PV power generator has the largest area of shading conditions of high power, the Parallel strings generator has the second largest, and the Long string generator has the smallest one. It could be anticipated that this is also the order of obtained total energy yield from these generator configurations under partial shading conditions. If we consider typical shading conditions with a shading strength of around 85%, Multi-string generator seems to provide still the largest overall energy yield. However, the order between the Long string and Parallel strings generators is not any more evident.

B. Mismatch Losses

Mismatch losses of the PV power generators have been calculated by comparing the power of the global MPP to the sum of the maximum powers of the individual blocks of 18 series-connected cells with one antiparallel-connected bypass diode. The mismatch losses in this case represent the lost power due to the fact that every block of PV cells does not operate in its own MPP, although the whole PV power generator operates in its global MPP. Mismatch losses are a characteristic property of each generator configuration. The mismatch losses of different PV power generators under partial shading conditions are shown in Fig. 7 as a function of system shading and shading strength as contour graphs.

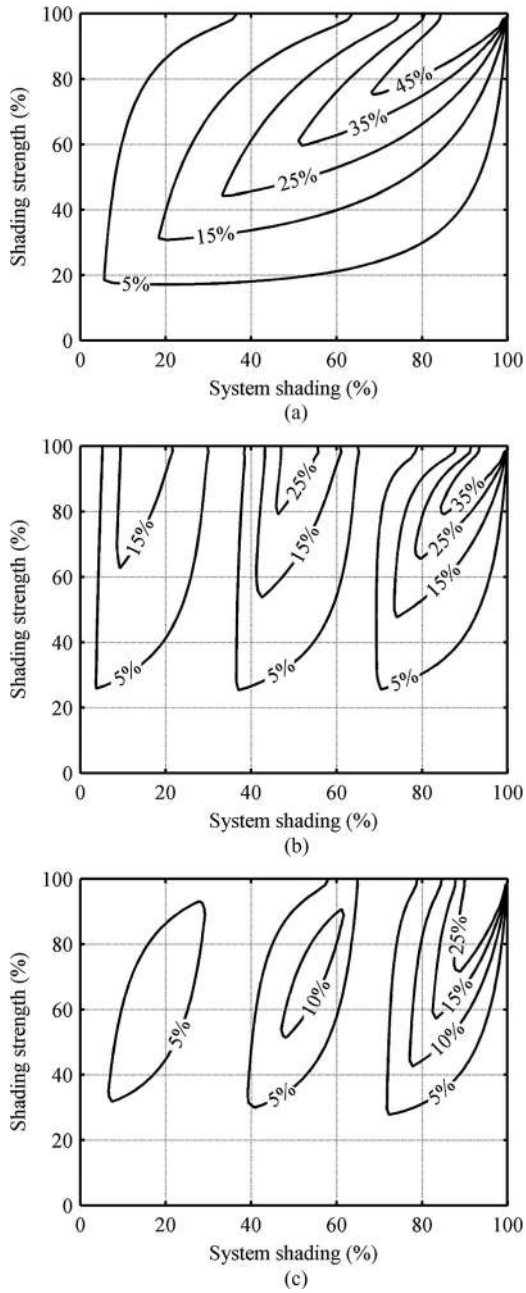

Fig. 7. Mismatch losses of PV power generators as a function of system shading and shading strength. (a) Long string, (b) Parallel strings, and (c) Multi-string generators. The mismatch losses are presented as the ratio of the power of the global MPP and the maximum available power that could be extracted if all the blocks of 18 series-connected PV cells would operate at their own MPPs.

Mismatch losses of the Long string generator are highest near the diagonal from origin to top-right corner of Fig. 7(a), where the powers of the two local MPPs, when both of them exist, are equal. As was explained earlier, power of the MPP at low voltages decreases as system shading increases and the power of the MPP at high voltages decreases as shading strength increases. On the diagonal of Fig. 7(a), the powers of the MPPs are equal, which leads to high mismatch losses, because both the system shading and shading strength are equally high. For Parallel strings and Multi-string generators, three different partial

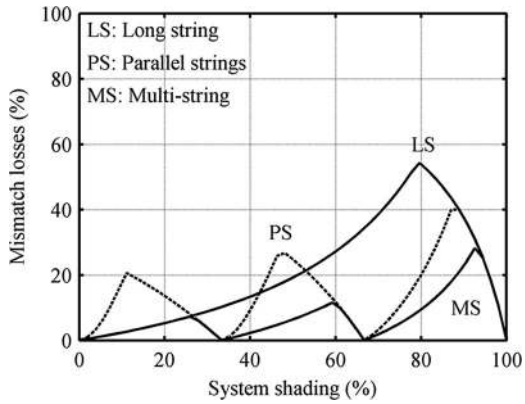

Fig. 8. Mismatch losses of the PV power generators under partial shading conditions as a function of system shading for shading strength of 85%.

shading conditions lead to two local MPPs with equal powers as can been seen in Fig. 7(b) and (c), because of three parallel operating series strings. The mismatch losses are almost zero when every string is either completely non-shaded or shaded, and therefore, the whole PV power generator is operating under uniform conditions. These conditions can be seen in Fig. 7(b) and (c) for system shadings of 33.3% or 66.7%.

Mismatch losses in case of the Long string generator can be considerable if both the system shading and shading strength are very high as can be seen in top-right corner of Fig. 7(a). In general, mismatch losses are lower for the Parallel strings and Multi-string generators than for the Long string generator and lowest for the Multi-string generator. In certain partial shading conditions, the mismatch losses in the Long string generator are considerable, while they are almost zero for the other two generators as can be seen, for example, for system shadings of 33.3% and 66.7% in Fig. 7.

When a PV power generator operates under partial shading conditions, the direct part of the solar radiation is blocked from reaching the PV modules and only the diffuse part of the global radiation is received by the shaded modules. On a clear sky day, the diffuse part of the radiation is typically about 15–20% of the global radiation [32]. The mismatch losses of the different PV power generators under partial shading conditions for shading strength of 85% are illustrated in Fig. 8 as a function of system shading. The curves in the figure are cross cuttings from Fig. 7(a)–(c).

As shown in Fig. 8, the mismatch losses of the Multi-string generator on a clear sky day are never higher than for the Long string or Parallel strings generators. Mismatch losses for Parallel strings are mostly lower than for the Long string generator. Mismatch losses for Parallel strings are higher than for Long string generator predominantly in case when shading strength is higher than 50% and system shading is low as can be seen by comparing mismatch losses in Fig. 7(a) and (b). This can most clearly be seen for shading strength of 85% in Fig. 8 for system shadings below 26% (first peak of the Parallel strings curve) and around 48% (second peak of the Parallel strings curve). For system shading of 11%, the mismatch losses for Parallel strings are 21%, whereas the mismatch losses for the Long string and

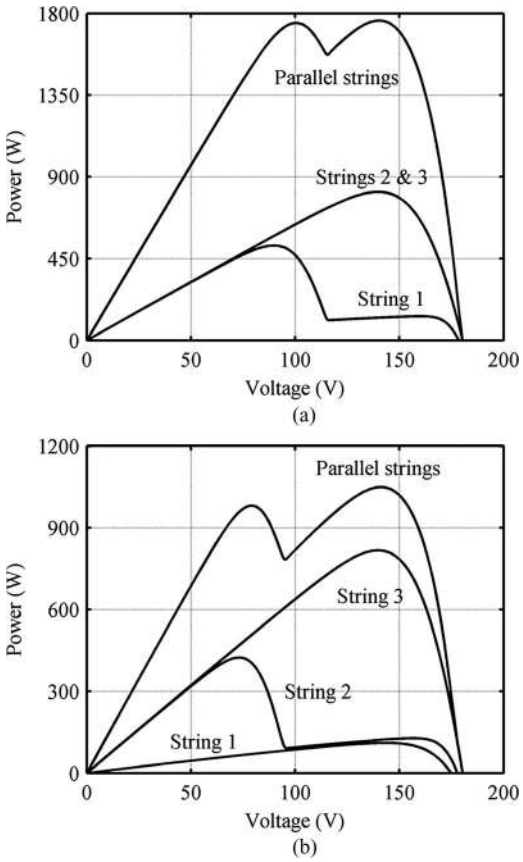

Fig. 9. *P–U* curves of the Parallel strings generator and individual curves of parallel-connected Strings 1, 2, and 3 under partial shading conditions with shading strength of 85% and system shadings of (a) 11% and (b) 48%.

Multi-string generators are only 3%. For system shading of 48%, the mismatch losses for Parallel strings are 27%, whereas the mismatch losses for the Long string and Multi-string generators are only 18% and 6%, respectively.

The *P–U* curve of the Parallel strings generator and individual *P–U* curves of the three parallel-connected strings are shown in Fig. 9 for shading strength of 85% and system shadings of 11% and 48%. As can be seen in Fig. 9(a) for system shading of 11%, two strings are without shading and String 1 operates under partial shading conditions. The global MPP of the generator is at 140 V, where String 1 has a power of 125 W. However, the global MPP of String 1 is around 90 V with a power of 525 W. In this case, the mismatch losses are 470 W and 21% of the power that could be extracted if every block of PV cells would operate at its own global MPP. In the case of system shading of 48% in Fig. 9(b), String 1 is completely shaded, String 2 is under partial shading conditions, and String 3 is without shading. MPP voltages of Strings 1 and 3 are close to the global MPP voltage of the Parallel strings generator, but the voltage of the global MPP of String 2 is close to 73 V with power almost 300 W higher than at the local MPP at high voltages. Situation is the same as for String 1 in Fig. 9(a). The mismatch losses of the Parallel strings generator are as high as 27%, because the available power of the generator has decreased due to increased overall shading.

Reason for high mismatch losses of the Parallel strings generator at system shadings below 60% is that all the strings of the generator have the same voltage and, thereby, the local MPPs of the string under partial shading determines the MPP voltages of the whole generator. On the contrary, if the parallel strings are allowed to operate at their own MPPs according to the multistring generator configuration, mismatch losses are smallest for all shading conditions. When system shading increases to over 50%, the Long string generator has the highest mismatch losses, the Parallel strings generator the second highest, and the Multi-string generator the lowest losses.

Mismatch losses of different PV power generator configurations presented in this paper have also been previously studied in [33]. Three scenarios were used representing practical partial shading conditions during a typical sunny day for a PV power generator composed of 18 PV modules, which were installed in three adjacent module rows. Partial shading scenarios included a scenario with one PV module of the generator shaded the entire day, a scenario with mutual shading of the PV module rows on the morning after the sunrise and in the afternoon before sunset, and a scenario with a large object such as a building starting to shade the PV power generator in the afternoon.

According to [33], the Multi-string generator had the lowest mismatch energy losses from 1% to 4% in all of the three partial shading scenarios and the Long string generator had only slightly higher losses. The Parallel strings generator had the highest mismatch losses between 3% and 9%. On a clear sky day, the mismatch losses due to mutual shading of the PV module rows were highest for all generator configurations having values between 3% and 9% and the Parallel strings generator had the highest losses.

C. Power Difference of the Local MPPs

Mismatch losses are not the only losses under partial shading conditions caused by the interconnection of PV modules. There can also be losses due to the fact that under partial shading conditions, the *P–U* curve of the PV generator has typically multiple MPPs and the generator can operate in a local MPP of low power instead of the global MPP. From MPP tracking point of view, multiple MPPs are troublesome, because conventional MPP tracking algorithms based on hill climbing type of methods are not able to track the global MPP in case of multiple MPPs. The conventional MPP tracking algorithms track always the closest local MPP. From this point of view, the power difference of the local MPPs under partial shading conditions is important when choosing the configuration for the PV power generator, if a conventional MPPT algorithm will be implemented.

The power difference of local MPPs for the studied PV power generators for shading strength of 85% is shown in Fig. 10 relatively to the power of the global MPP, P_{GMPP}. The relative power difference is calculated by using the absolute value of the power difference, because we are mainly interested on the magnitude of the power difference. In case of two local MPPs, P_{MPP1} is the power of the local MPP at low voltages and P_{MPP2} is the power of the MPP at high voltages. The power difference

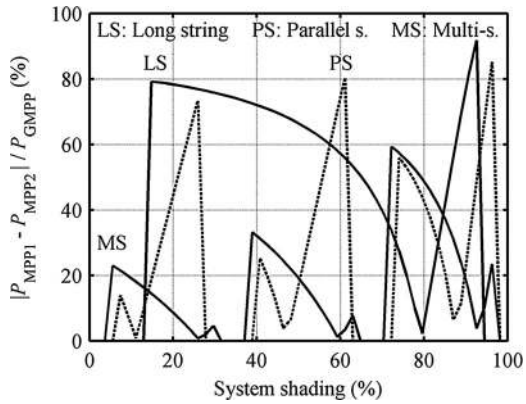

Fig. 10. Relative power differences of local MPPs as a function of system shading for different generators for shading strength of 85% (corresponding to the diffuse irradiance on a clear sky day).

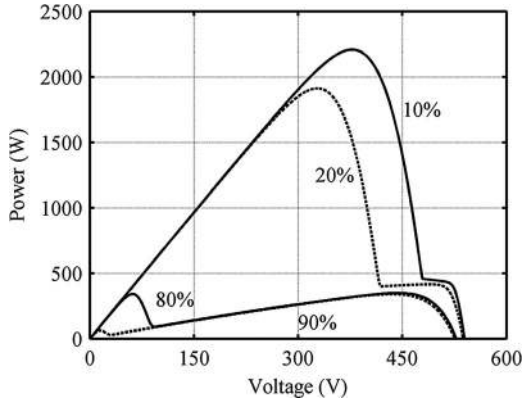

Fig. 11. *P–U* curves of the Long string generator under partial shading conditions with shading strength of 85% and with system shadings of 10%, 20%, 80%, and 90%.

is zero in cases of only one MPP and when the powers of the local MPPs are equal.

For the Long string generator, there is only one MPP when system shading is less than 13% or more than 94% (see Fig. 10). The powers of the local MPPs are almost equal when system shading is 80%. The reason, why the power difference is not exactly zero, is that the system shading has discrete steps in the simulations. Therefore, the powers of the local MPPs are never exactly the same for the studied shading strengths. For Parallel strings generator, there is only one MPP when system shading is less than 6%, 28–39%, 63–72%, or more than 98%. The powers of the local MPPs are almost equal when system shading is 11%, 46%, or 87%. Three similar patterns are repeated with increasing system shading for Parallel strings generator because there are three different strings from which only one is under partial shading conditions at a time. This applies also to the Multi-string generator. For Multi-string generator, there is only one MPP when system shading is less than 4%, 32–37%, 65–70%, or more than 98%. The powers of the local MPPs are practically equal when system shading is 26%, 59%, or 93%.

The relative power differences of the local MPPs are as high as 80% or 92% for the Long string generator in Fig. 10 for system shadings of 15% or 93%, respectively. For these conditions, the power lost due to the tracking of the MPP with lower power than the global one is considerable. For Parallel strings generator, the relative power difference has maximum values of around 80% at system shadings of 26%, 61%, and 96%. The power difference pattern in Fig. 8 repeats itself three times, once due to partial shading of each parallel string. For Multi-string generator, the pattern also repeats itself with increasing system shading, once for each parallel string. The maximum values of the relative power differences are at system shadings of 6%, 39%, and 72% having considerably lower values than for other generators.

Tracking of the local MPP with lower power causes in most cases largest power losses for the Long string generator, because of the wide system shading region from 13% to over 50% with high relative power difference between the local MPPs. For system shading of around 80%, the power lost due to tracking of wrong MPP is close to zero for the Long string generator. However, it should be noticed that the mismatch losses are 54% for the Long string generator at that point, as can be seen in Fig. 8, while for the other generators, they are considerably less. Therefore, the power of the global MPP is only 46% of the maximum available power for the Long string generator for shading strength of 85% and system shading of 80%. The mismatch losses for the Parallel strings generator in these conditions are 20% and the power lost due to tracking of a local MPP with lower power is 43%. The total power loss is then 54% of the available maximum power, which is the same as for the Long string generator in these conditions.

For system shading of less than 13%, power is lost due to the tracking of the local MPP with lower power only in Parallel strings and Multi-string generators (see Fig. 10). In these conditions, the Long string generator has only one MPP. This indicates that for objects shading only a small portion of the PV power generator, the Long string generator is less affected regardless of the MPPT algorithm. Although the power lost due to tracking of a local MPP with lower power instead of the global MPP is higher for Multi-string generator than for Parallel strings generator for some system shading strengths, the mismatch losses are much higher for Parallel strings generator (see Fig. 8). Therefore, more power can be yielded from Multi-string than from Parallel strings generator.

In order to illustrate the effects of different partial shading conditions, *P–U* curves of the Long string generator are shown in Fig. 11 for shading strength of 85% and system shadings of 10%, 20%, 80%, and 90%. In case of 10% system shading, there is only one MPP at 380 V although there is a step on the curve at voltages around 500 V. With increasing system shading, this step becomes a local MPP. For 20% system shading, there are already two MPPs, a global one at 330 V and another at 500 V. The power difference of these local MPPs is about 1500 W yielding to high losses if the MPP at 500 V is tracked as might happen in case of conventional MPPT algorithms. For system shading of 80%, the powers of the local MPPs are almost equal both being under 400 W. In this case, the power lost due to the tracking of the local MPP instead of the global one does not lead to high losses, whereas the mismatch losses are high as can

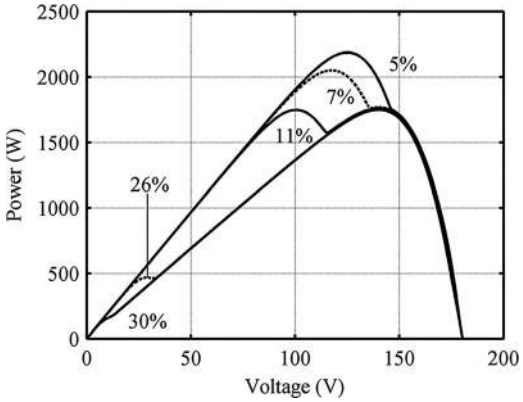

Fig. 12. *P–U* curves of the Parallel strings generator under partial shading conditions with shading strength of 85% and with system shadings of 5%, 7%, 11%, 26%, and 30%.

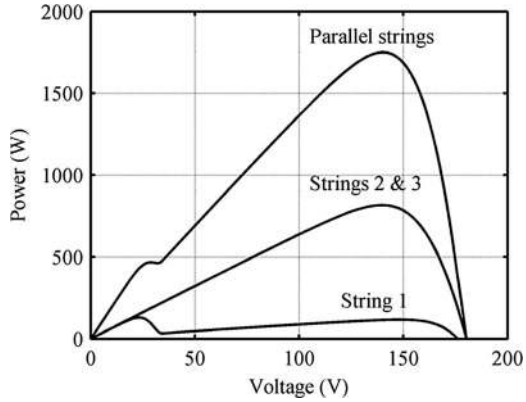

Fig. 13. *P–U* curve of the Parallel strings generator and individual curves of parallel-connected Strings 1, 2, and 3 under partial shading conditions with shading strength of 85% and with system shading of 26%.

be seen in Fig. 8. For system shading of 90%, the power of the local MPP at 10 V is much lower than the power of the global MPP at 450 V. Although the power of the global MPP is quite low, tracking of the MPP at 10 V leads to high relative power losses.

The *P–U* curves of the Parallel strings generator are shown for shading strength of 85% and system shadings of 5%, 7%, 11%, 26%, and 30% in Fig. 12. In case of system shading of 5%, there is only one MPP at 125 V although there is a step in the curve at voltages around 150 V. For system shading of 7%, the step on the 5% curve has become a local MPP at 140 V and the global MPP is at 120 V. The power difference of these local MPPs is about 300 W yielding to considerable losses if the MPP at 140 V is tracked as might happen in case of conventional MPPT algorithms. For system shading of 11%, the powers of the MPPs are practically equal and tracking the MPP with lower power does not cause power losses, but the mismatch losses are at maximum of 21% for Parallel strings generator (see Fig. 8). For system shading of 26%, the relative power difference of the local MPPs has a local maximum value of 73% having an absolute power loss of 1280 W. In this case, the power lost due to tracking of the local MPP with lower power leads to high losses, whereas the mismatch losses are quite low as can be seen in Fig. 8. With increasing system shading, the local MPP at low voltages disappears being only a step at 30% curve. The behavior of the *P–U* curves is qualitatively quite similar also for the two other patterns of the Parallel strings generator at higher systems shadings (see Fig. 10), because the same basic phenomenon takes place in each of the strings with increasing system shading.

The *P–U* curve of the Parallel strings generator corresponding to system shading of 26% has the maximum difference between the powers of the local MPPs (see Figs. 10 and 12). It is shown in Fig. 13 with the curves of the individual strings connected in parallel to further demonstrate the cause for the large difference between local MPP powers. As can be seen, two strings are operating under uniform conditions and one under partial shading conditions with two MPPs, which have almost equal low powers at different voltages.

In the case of Multi-string generator, parallel strings do not have the same operating voltage, which allows them to operate at their global MPPs. In these cases, the behavior of their *P–U* curves can be deduced from the *P–U* curves of the Long string generator in Fig. 11. The same phenomenon happens for each parallel string as for the Long string, but three times with increasing system shading having maximum power difference between MPPs of only one-third compared to the Long string generator.

V. Conclusion

The effects of partial shading on Long string, Parallel strings, and Multi-string PV power generators have been investigated by using an experimentally verified simulation model based on the well-known one-diode model of a PV cell. Partial shading was varied with respect to system shading and shading strength, which represent the amount of shaded PV modules of the generator, and the attenuation of the irradiance due to the shading, respectively. The effects of partial shading was studied on the power of the global MPP of the generators, on the mismatch losses caused by operating at the global MPP, which differs from the sum of the maximum powers of individual blocks of PV cells with antiparallel-connected bypass diode, and on operating at a local MPP instead of the global one in case of multiple MPPs.

The results clearly show that the PV power generator composed of a long series connection of PV modules is more prone to reduction of maximum power, increase of mismatch losses, and losses due to failure in tracking the global MPP under partial shading conditions than the configurations with short strings connected in parallel or short strings controlled individually as in the Multi-string generator. Short strings controlled individually seem to be the best generator configuration on the power production point of view in case of partial shading conditions. On the other hand, if the PV power generator is designed so that only a small portion of the generator can be shaded at a time, the Long string generator has as low mismatch losses as the Multi-string generator and no losses due to failure in MPP

tracking, because of only one MPP in the *P–U* characteristic of the generator.

Based on the results shown in this paper, both series and parallel connections should be, in general, minimized in order to increase the energy yield of PV power generators that are prone to partial shading conditions. This is especially important for building-integrated PV power generators and generators operating in built environments. Also, shading due to climatic conditions can be of importance for PV power generation.

REFERENCES

[1] A. Jäger-Waldau, "Photovoltaics and renewable energies in Europe," *Renewable Sustainable Energy Rev.*, vol. 11, no. 7, pp. 1414–1437, Sep. 2007.

[2] S. Rahman, "Green power: What is it and where can we find it?," *IEEE Power Energy Mag.*, vol. 1, no. 1, pp. 30–37, Jan./Feb. 2003.

[3] B. Bose, "Global warming: Energy, environmental pollution, and the impact of power electronics," *IEEE Ind. Electron. Mag.*, vol. 4, no. 1, pp. 6–17, Mar. 2010.

[4] B. Kroposki, R. Margolis, and D. Ton, "Harnessing the sun," *IEEE Power Energy Mag.*, vol. 7, no. 3, pp. 22–32, May/Jun. 2009.

[5] M. Liserre, T. Sauter, and J. Y. Hung, "Future energy systems: Integrating renewable energy sources into the smart power grid through industrial electronics," *IEEE Ind. Electron. Mag.*, vol. 4, no. 1, pp. 18–37, Mar. 2010.

[6] J. A. Gow and C. D. Manning, "Photovoltaic converter system suitable for use in small scale stand-alone or grid connected applications," *IEE Proc.—Electr. Power Appl.*, vol. 147, no. 6, pp. 535–543, Nov. 2000.

[7] C. Lashway, "Photovoltaic system testing techniques and results," *IEEE Trans. Energy Convers.*, vol. 3, no. 3, pp. 503–506, Sep. 1988.

[8] E. Molenbroek, D. W. Waddington, and K. A. Emery, "Hot spot susceptibility and testing of PV modules," in *Proc. Conf. Rec. 22nd IEEE Photovoltaic Spec. Conf.*, 1991, vol. 1, pp. 547–552.

[9] S. Silvestre, A. Boronat, and A. Chouder, "Study of bypass diodes configuration on PV modules," *Appl. Energy*, vol. 86, no. 9, pp. 1632–1640, Sep. 2009.

[10] T. Esram and P. L. Chapman, "Comparison of photovoltaic array maximum power point tracking techniques," *IEEE Trans. Energy Convers.*, vol. 22, no. 2, pp. 439–449, Jun. 2007.

[11] V. Salas, E. Olías, A. Barrado, and A. Lázaro, "Review of the maximum power point tracking algorithms for stand-alone photovoltaic systems," *Solar Energy Mater. Solar Cells*, vol. 90, no. 11, pp. 1555–1578, Jul. 2006.

[12] K. Kobayashi, I. Takano, and Y. Sawada, "A study of a two stage maximum power point tracking control of a photovoltaic system under partially shaded insolation conditions," *Solar Energy Mater. Solar Cells*, vol. 90, pp. 2975–2988, Nov. 2006.

[13] R. Alonso, P. Ibánez, V. Martínez, E. Román, and A. Sanz, "An innovative perturb, observe and check algorithm for partially shaded PV system," in *Proc. 13th Eur. Conf. Power Electron. Appl.*, Barcelona, Spain, 2009, pp. 1–8.

[14] C. E. Chamberlin, P. Lehman, J. Zoellick, and G. Pauletto, "Effects of mismatch losses in photovoltaic arrays," *Solar Energy*, vol. 54, no. 3, pp. 165–171, Mar. 1995.

[15] S. Silvestre and A. Chouder, "Effects of shadowing on photovoltaic module performance," *Prog. Photovoltaic: Res. Appl.*, vol. 16, no. 2, pp. 141–149, Sep. 2007.

[16] V. Quaschning and R. Hanitsch, "Numerical simulation of current-voltage characteristics of photovoltaic systems with shaded solar cells," *Solar Energy*, vol. 56, no. 6, pp. 513–520, Jun. 1996.

[17] M. C. Alonso-García, J. M. Ruiz, and F. Chenlo, "Experimental study of mismatch and shading effects in the I-V characteristic of a photovoltaic module," *Solar Energy Mater. Solar Cells*, vol. 90, no. 3, pp. 329–340, Feb. 2006.

[18] N. D. Kaushika and A. K. Rai, "An investigation of mismatch losses in solar photovoltaic cell networks," *Energy*, vol. 32, no. 5, pp. 755–759, May 2007.

[19] E. Karatepe, M. Boztepe, and M. Çolak, "Development of a suitable model for characterizing photovoltaic arrays with shaded solar cells," *Solar Energy*, vol. 81, no. 8, pp. 977–992, Aug. 2007.

[20] G. Walker, "Evaluating MPPT converter topologies using a MATLAB PV model," *J. Electr. Electron. Eng.*, vol. 21, no. 1, pp. 49–56, 2001.

[21] A. Mäki, S. Valkealahti, and J. Leppäaho, "Operation of series-connected silicon-based photovoltaic modules under partial shading conditions," *Prog. Photovoltaic: Res. Appl.*, doi: 10.1002/pip.1138, to be published.

[22] R. E. Hanitsch, D. Schulz, and U. Siegfried, "Shading effects on output power of grid connected photovoltaic generator systems," *Rev. Energy Ren.: Power Eng.*, vol. 4, pp. 93–99, 2001.

[23] M. A. Gross, S. O. Martin, and N. M. Pearsall, "Estimation of output enhancement of a partially shaded BIPV array by the use of AC modules," in *Proc. Conf. Rec. 26th IEEE Photovoltaic Spec. Conf.*, Anaheim, CA, 1997, pp. 1381–1384.

[24] E. V. Paraskevadaki and S. A. Papathanassiou, "Evaluation of MPP voltage and power of mc-Si PV modules in partial shading conditions," *IEEE Trans. Energy Convers.*, vol. 26, no. 3, pp. 923–932, Sep. 2011.

[25] A. Woyte, J. Nijs, and R. Belmans, "Partial shadowing of photovoltaic arrays with different system configurations: Literature review and field test results," *Solar Energy*, vol. 74, no. 3, pp. 217–233, Mar. 2003.

[26] F. Schimpf and L. E. Norum, "Grid connected converter for photovoltaic, state of the art, ideas for improvement of transformerless inverters," presented at the Nordic Workshop Power Ind. Electron., Espoo, Finland, Jun. 9–11, 2008.

[27] M. García, J. M. Maruri, L. Marroyo, E. Lorenzo, and M. Pérez, "Partial shadowing, MPPT performance and inverter configurations: Observations at tracking PV plants," *Prog. Photovoltaic: Res. Appl.*, vol. 16, no. 6, pp. 529–536, Apr. 2008.

[28] M. G. Villalva, J. R. Gazoli, and E. R. Filho, "Comprehensive approach to modeling and simulation of photovoltaic arrays," *IEEE Trans. Power Electron.*, vol. 24, no. 5, pp. 1198–1208, May 2009.

[29] S. Liu and R. A. Dougal, "Dynamic multiphysics model for solar array," *IEEE Trans. Energy Convers.*, vol. 17, no. 2, pp. 285–294, Jun. 2002.

[30] S. R. Wenham, M. A. Green, M. E. Watt, and R. Corkish, "The behaviour of solar cells," in *Applied Photovoltaics,* 2nd ed. London, U.K.: Earthscan, 2007, pp. 43–56.

[31] J. Dunlop, "Cells, modules, and arrays," in *Photovoltaic Systems.* Homewood, IL: Amer. Tech. Publishers, 2005, pp. 128–138.

[32] S. Armstrong and W. G. Hurley, "A new methodology to optimise solar energy extraction under cloudy conditions," *Renew. Energy*, vol. 35, no. 4, pp. 780–787, Apr. 2010.

[33] A. Mäki and S. Valkealahti, "Operation of long series-connected silicon-based photovoltaic module string and parallel-connected short strings under partial shading conditions," in *Proc. 26th Eur. Photovoltaic Solar Energy Conf. Exhib.*, Hamburg, Germany, 2011, pp. 4227–4232.

Anssi Mäki (S'09) was born in Kauhava, Finland, 1985. He received the M.Sc. degree in electrical engineering from the Tampere University of Technology, Tampere, Finland, in 2010.

He has been with the Department of Electrical Energy Engineering, Tampere University of Technology as a Researcher, pursuing for the doctoral degree since the beginning of 2010. His current research interests include the operation of photovoltaic power generators and the development of maximum power point tracking algorithms.

Mr. Mäki is a member of IEEE Power and Energy Society.

Seppo Valkealahti (M'10) was born in Alavus, Finland, 1955. He received the M.Sc. and Ph.D. degrees in physics from the University of Jyväskylä, Jyväskylä, Finland, in 1983 and 1987, respectively.

From 1982 to 1997, he was a Teacher and Researcher of physics at the University of Jyväskylä, in the Riso National Laboratory in Denmark and in the Brookhaven National Laboratory in Upton, NY. From 1997 to 2004, he worked in ABB heading research and product development activities. In the beginning of 2004, he joined the Tampere University of Technology, Tampere, Finland, where he is currently a Professor in the Department of Electrical Energy Engineering. His research interests include electric power production and consumption-related technologies, solar energy, and multiscientific problems related to power engineering.

Dr. Valkealahti is a member of IEEE Power and Energy Society.